

Nonlinear Finite Element Analysis of Thin-Walled Beam on Pre- and Post-Buckling Stiffness and Gauge Sensitivity Index

Shengyong Zhang

Department of Mechanical and Civil Engineering, College of Engineering and Sciences, Purdue University Northwest, Hammond, USA

Email: syzhang@pnw.edu

How to cite this paper: Zhang, S.Y. (2022) Nonlinear Finite Element Analysis of Thin-Walled Beam on Pre- and Post-Buckling Stiffness and Gauge Sensitivity Index. *Journal of Applied Mathematics and Physics*, 10, 1432-1442.

<https://doi.org/10.4236/jamp.2022.105101>

Received: March 24, 2022

Accepted: May 7, 2022

Published: May 10, 2022

Copyright © 2022 by author(s) and Scientific Research Publishing Inc. This work is licensed under the Creative Commons Attribution International License (CC BY 4.0).

<http://creativecommons.org/licenses/by/4.0/>



Open Access

Abstract

Lightweight design has a significant impact on reducing fuel consumption and harmful emission of conventional vehicles and improving driving range of electric vehicles. Reducing the thickness of components in vehicle bodies and closures is an efficient approach for weight reduction. Thickness reduction, however, will reduce structural stiffness, especially in the presence of lateral displacements of buckling when critical stress is reached. In this paper, nonlinear FEA models of a thin-walled beam with variable thickness are developed for calculating the changes of beam stiffness as to thickness reduction in the pre- and post-buckling stages. Next, these stiffness values are used to calculate gauge sensitivity of the beam, which changes with respect to beam thickness changes. It is concluded that the presence of buckling will reduce the beam stiffness, worsen the stress uniformity, and increase the gauge sensitivity value of the beam.

Keywords

FEA, Local Buckling, Gauge Sensitivity, Thin-Walled Structures

1. Introduction

Lightweight design has been a promising approach for reducing fuel consumption and harmful emission of vehicles with conventional powertrains and improving driving range of vehicles with electric powertrains. Kim and Wallington [1] [2] developed physics-based models to formulate the relationship between vehicle weight and mass-dependent fuel consumption based on vehicle dynamics theories with parameters including rolling, rotating, and acceleration loads.

Braking energy via regenerative braking system in electric vehicles, which has an effect similar to weight reduction, was taken into account in the developed simulation models. The mass-induced fuel consumption (MIF) and fuel reduction values (FRVs) were computed and compared for 13 conventional vehicles and 37 electric vehicles. Geyer and Malen [3] [4] analyzed the energy demand for vehicles with conventional, battery electric, and series plug-in hybrid electric powertrains. The simulation models were based on driving and powertrain dynamics by calculating the force required of the driving wheels and the corresponding torque and rotating velocity transmitted through powertrains. The regenerative braking energy and battery charging/discharging losses were considered in the models. It was concluded that the change in vehicle energy demand due to mass reduction (MJ per 100 km driven and per 100 kg reduction) was smaller for pure electric vehicles due to their efficient powertrains, compared to those of conventional vehicles. Electric vehicles are usually heavier than similar conventional vehicles due to the batteries, sensors, and infotainment systems, and are restricted to short-distance commutes only. Lightweight electric vehicles reduce the battery consumption and lower the battery capacity, yielding an improvement of driving range under the same driving conditions [5]. In summary, lightweighting remains a crucial approach for reducing fuel consumption and harmful emission of conventional vehicles and improving driving range of electric vehicles.

Prevailing approaches for reducing vehicle weight include substitution of materials (high-strength steels, aluminum alloys, composites, etc.), advanced manufacturing technologies (additive manufacturing, laser welding, high-pressure die casting, etc.), and optimal structural designs (size, shape, topology optimization, etc.). Bai *et al.* [6] proposed a bridging method to transform topologically optimized vehicle frame structures into thin-walled frame structures. The thin-walled cross-sectional properties were designed by referring to the solid cross sections from topological optimum results. Further size and shape optimization was conducted for lightweight design under constraints of structural stiffness and manufacturing requirements. Czerwinski [7] assessed the current trends and technologies in lightweight vehicle design. It was stated that except of structural efficiency, material substitutions represent a key part in current lightweighting strategies for optimizing structures, maximizing weight reductions, and fulfilling required performance and safety standards. The importance of steels, especially the advanced high-strength steel (AHSS) with very high tensile strength, had been emphasized in this paper due to their advantages over nonferrous alloys on material price, manufacturability, and sustainability. Burd *et al.* [8] compared the AHSS and aluminum alloys in their applications for lightweight design of electric vehicle bodies and closures. Cost analysis was conducted for material substitution with AHSS and aluminum alloys. It was illustrated that application of AHSS will reduce the manufacturing and assembly cost, while application of aluminum alloy will have advantage on battery and motor cost. Steels remains as a cost-effective material for fabricating vehicle bodies and closures. Steels have

exceptional strength, ductility and stiffness combinations which ensure occupant safety and achieve satisfied noise, vibration and harshness (NVH) control. Excellent formability of steels, aligned with existing manufacturing technologies, allows and facilitates architectural innovative designs of vehicle frames. The availability of high-strength steel, advanced high-strength steel and ultra-high-strength steel grades provides automobile designers the option of incorporating more thin-walled components in vehicle bodies and closures for weight reduction. One advantage of thin-walled components lies in high material effectiveness which results in high stiffness-to-weight ratio. However, thickness reduction will result in stiffness reduction of components. When critical stress is reached, the component stiffness will be reduced further due to the onset of lateral displacements of buckling [9] [10]. In this paper, nonlinear FEA has been conducted to investigate the stiffness changes of a thin-walled beam in pre-buckling and post-buckling stages. Gauge sensitivity, derived from stiffness-related parameters for accessing the effect of thickness change on structural performance, is calculated for the beam with different thickness for validating the effect of buckling. It is illustrated that the presence of buckling will reduce the beam stiffness, worsen the stress uniformity, and increase the gauge sensitivity value of the beam. In Section 2, the concept of gauge sensitivity index is reviewed, and the effect of local buckling on gauge sensitivity values is illustrated. In Section 3, nonlinear FEA models of a thin-walled beam with variable thickness are developed for calculating the changes of beam stiffness with respect to thickness changes in the pre- and post-buckling stages. The effect of local buckling on the beam gauge sensitivity has been validated based on the obtained stiffness values. Finally, conclusions are drawn.

2. Gauge Sensitivity Concept

Gauge sensitivity index was developed to assess the effect of thickness changes on stiffness-related parameters of thin-walled beams [11] [12]. The derivation was based on the cross-sectional moment of inertia of a hypothetical twin-flange cantilevered beam with negligible web elements. For a cantilever beam, it can be validated that the webs resist most of the transverse shear force, while the flanges resist most of the bending moment experienced by the beam. Gauge sensitivity index, λ , was derived by ignoring the webs as

$$\lambda = \frac{I'}{I/t} \quad (1)$$

where I is the cross-sectional moment of inertia and I' is the derivative of I with respect to the characteristic thickness t . It is concluded based on the hypothetical twin-flange beam that λ changes from 3 for thick-walled beams to 1 for thin-walled beams.

Figure 1 shows a beam with closed-hat cross section whose λ can be expressed as a function of thickness based on its cross-sectional moment of inertia using Equation (1) by

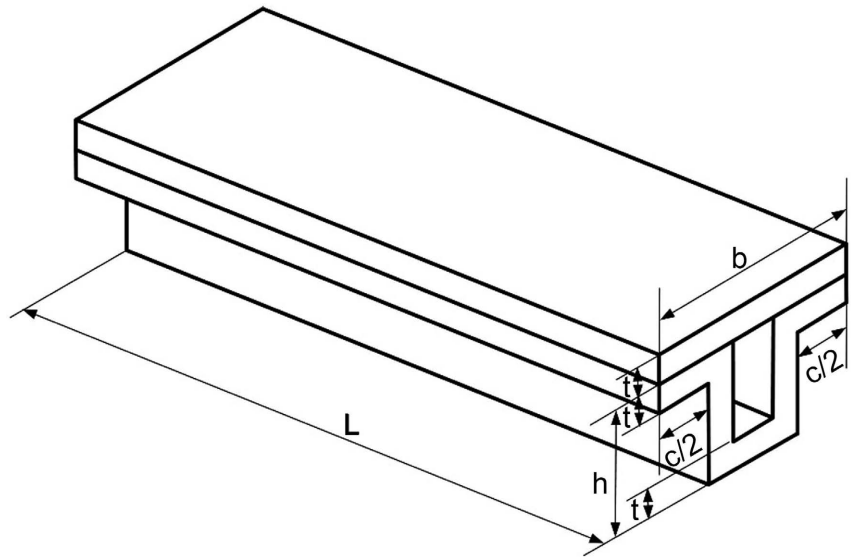


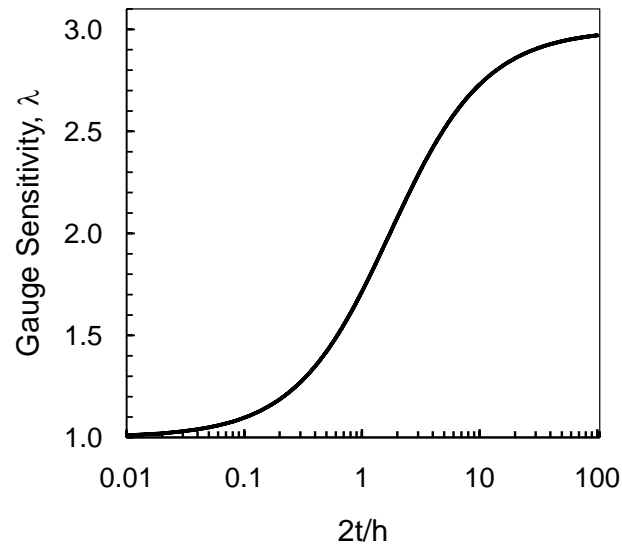
Figure 1. Beam with closed-hat cross section.

$$\lambda = \frac{\frac{3}{2} \left(\frac{3 \left(1 - \left(\frac{c}{b} \right)^2 \right) + 4 \left(\frac{h}{b} \right) + \left(\frac{h}{b} \right)^2}{6 \left(1 + \left(\frac{h}{b} \right) \right)} + 3 \left(1 - \left(\frac{c}{b} \right) \right) \left(\frac{t}{h} \right) + 3 \left(\frac{t}{h} \right)^2}{\frac{3}{2} \left(\frac{3 \left(1 - \left(\frac{c}{b} \right)^2 \right) + 4 \left(\frac{h}{b} \right) + \left(\frac{h}{b} \right)^2}{6 \left(1 + \left(\frac{h}{b} \right) \right)} + \frac{3}{2} \left(1 - \left(\frac{c}{b} \right) \right) \left(\frac{t}{h} \right) + \left(\frac{t}{h} \right)^2} \quad (2)$$

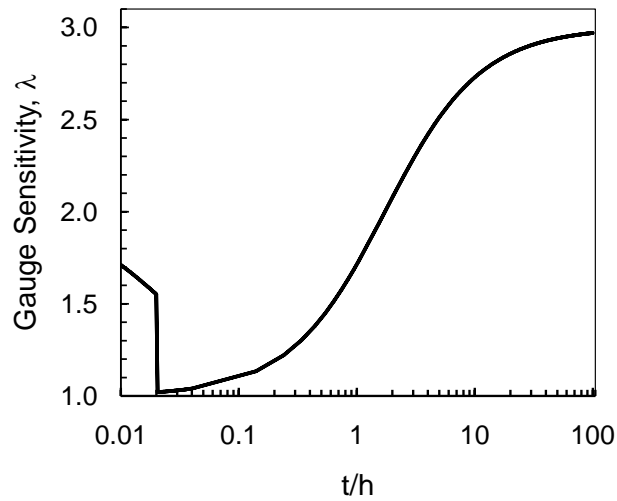
where b represents the width of the flange, h the height, c the lip length, and t the thickness.

Thin-walled beams have advantages over thick-walled beams on the effectiveness of material usage. Materials in a thin-walled beam tend to be efficiently loaded, resulting in near-uniform internal resultant loading distributions in the beam. λ value of 1 indicates thin-walled beams have high material effectiveness and high stiffness-to-weight ratio. With increasing of thickness, the internal load distribution in the beam changes to be more and more nonuniform due to the requirements for maintaining static equilibrium states. Correspondingly, λ values increase from 1 up to 3 for thick-walled beams as shown in **Figure 2(a)**.

λ value of 1 is important but it has not embodied the effect of buckling when the wall thickness becomes very thin. For a beam with very thin sections, local buckling may occur in the compressive components when critical stress is reached. The buckling manifests itself as a kind of out-of-plane deformation and creates a non-uniform longitudinal membrane stress distribution along the width of the components. The elastic post-buckling behavior is governed by equilibrium equations and compatibility equations. These equations may be solved by postulating a form of deflection and evaluating the corresponding stress function for



(a)



(b)

Figure 2. Variations of λ with respect to changes in component thickness. (a) Without buckling being present; (b) With buckling being present.

specified loadings and boundary conditions using the compatibility equations. Exact solutions can be attained by expressing the total potential energy in terms of stress and deflection functions and applying the principle of minimum potential energy. However, exact solutions are only available for some simple loading and constraint conditions. Alternative solutions based on the concept of effective width, developed by von Karman [9], have been applied to the design and analysis of cold-formed steel members in the post-buckling stage. The effective width method states that the ultimate load sustained by the compressive components does not increase in proportional to the actual width and is insensitive to variation in actual width when the critical stress is reached. With the onset of buckling, the membrane stress distribution will become nonuniform over the full width of the compression elements.

Gauge sensitivity index is a measurement of uniformity of internal loading distribution. λ value decreases as the thickness reduction proceeds in the pre-buckling stage. λ value of 1 indicates perfect uniform stress distribution. When buckling occurs in the compression elements, λ values are expected to increase accordingly, indicating an increasing of non-uniformity in stress distributions. Effective width method suggests replacing the post-buckling non-uniform stress by uniform stress distributed over the so-called effective width near supports. With decreasing in thickness, the flange which is in compression will lose its full effectiveness when the critical stress (75% of the material yielding strength in this study) is reached. Corresponding effective width of the flange is used in the calculation of its cross-sectional moment of inertia. The moment of inertia is a function of thickness and is subsequently used for calculating λ values. **Figure 2(b)** shows the variation of λ with respect to thickness changes. It is illustrated that the presence of buckling will lead to an increase in λ with the reduction of thickness.

3. Nonlinear FEA of Thin-Walled Beam for Pre- and Post-Buckling Performance

The beam with rectangular cross section as shown in **Figure 3** is analyzed for calculating the bending stiffness and gauge sensitivity at different thickness in the pre- and post-buckling stage. The beam is meshed using shell elements. One end of the beam is rigidly constrained. Forces being applied on the top flange and bottom flange at the other end have same magnitude but opposite direction, resulting in compressive stress and tensile stress in the top and bottom flanges, respectively.

FEA is conducted in three stages: linear structural analysis, eigenvalue buckling analysis, and nonlinear structural buckling analysis. Geometric model of the beam is meshed with shell elements in the linear FEA model with specified material properties. Two remote points are created at the loaded end of the beam through which compressive force and tensile force are applied to the top and bottom flanges, respectively. FEA data and results from the linear FEA analysis are input to the FEA linear eigenvalue buckling model for determination of buckling modes. Both linear static analysis and linear buckling analysis are configured

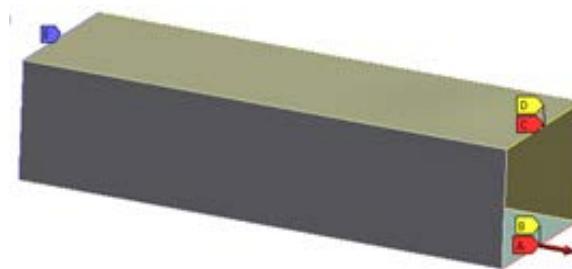


Figure 3. FEA model of a beam with a width of 75 mm, height of 52 mm, length of 225 mm, and variable thickness ranging from 10 mm to 1 mm. One end of the beam is rigidly fixed, and the other end is loaded.

and the mesh convergence analysis has been verified in this process. Based on the above FEA results, nonlinear structural buckling analysis is conducted in which the large deflection function is activated for evaluating the effect of buckling on beam stiffness. Beam thickness decreases progressively from 10 mm to 1 mm, with a decrement of 0.5 mm in this research. **Figure 4** shows the buckling deformation and non-uniform stress distribution in the post-buckling stage.

Bending moment is obtained by multiplying the applied force acting on one flange by the distance between the two flanges. The corresponding rotating angle of the line connecting the middle points of the two flanges, θ , is measured in the unit of radians as shown in **Figure 5**. In this study, the beam bending stiffness, k , is defined to be the quotient of the bending moment and corresponding rotating angle. Beam bending stiffness is plotted as a function of thickness that ranges from 10 mm to 1 mm in **Figure 6(a)**. For comparison, **Figure 6(a)** also shows the variation of beam bending stiffness without consideration of buckling effect in FEA modelling. It is found that the onset of compressive buckling reduces the bending stiffness further as to thickness reduction.

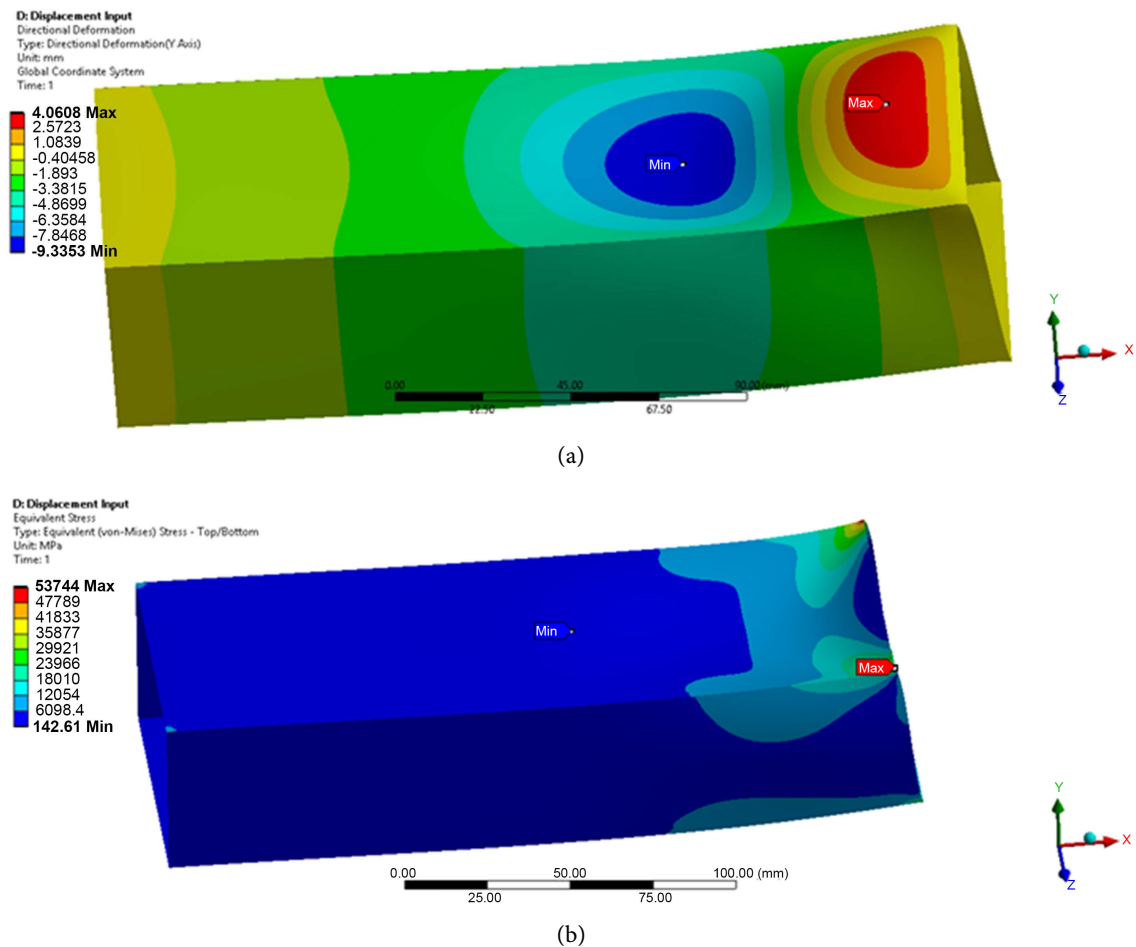


Figure 4. Buckling deformation and corresponding non-uniform stress distribution. (a) Deformation in the lateral direction in the post-buckling stage; (b) Non-uniform stress distribution with the presence of buckling in the compression flange.

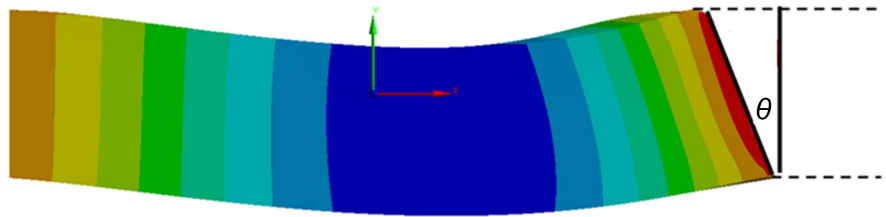
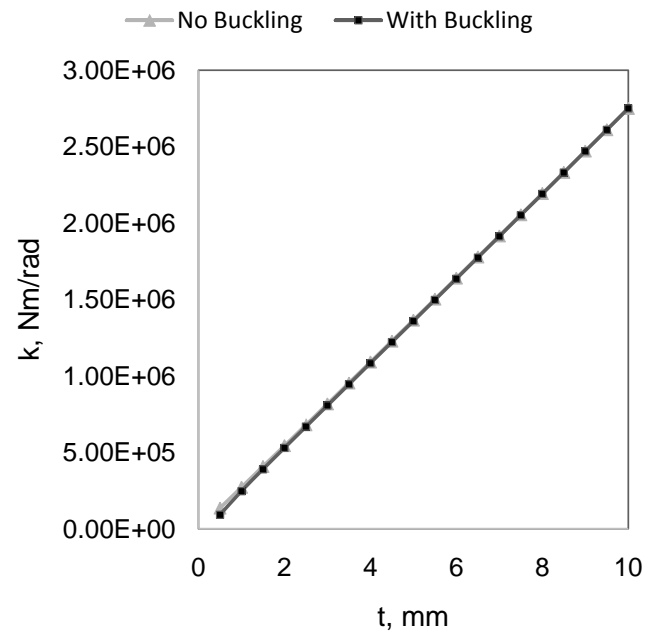
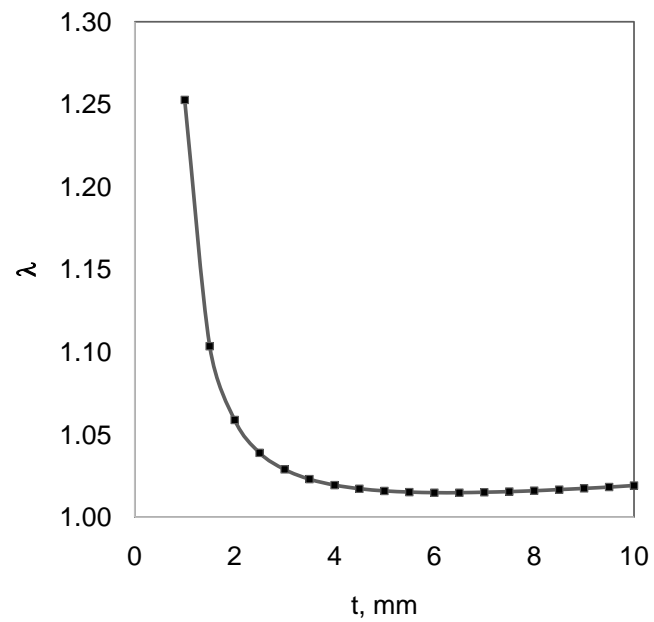


Figure 5. Rotating angle θ for calculating beam bending stiffness.



(a)



(b)

Figure 6. Variations of k and λ in the pre- and post-buckling stages. (a) Variations of bending stiffness; (b) Variations of gauge sensitivity.

λ value of the beam is calculated by replacing I in Equation (1) with beam bending stiffness as

$$\lambda = \frac{k'}{k/t} \quad (3)$$

For example, to calculate λ value at $t = 10$ mm, we substitute the k in the Equation (3) with the stiffness value at $t = 10$ mm, and the derivative of stiffness with respect to thickness, k' , is approximated by dividing the stiffness change at $t = 10$ mm and $t = 9.5$ mm by the thickness change, which is 0.5 mm. Similarly, to calculate λ value at $t = 9.5$ mm, the derivative of stiffness in Equation (3) is approximated by dividing the stiffness change at $t = 9.5$ mm and $t = 9.0$ mm by the thickness change, which is 0.5 mm again, and so forth.

In the pre-buckling stage corresponding to thickness change from 10 mm to around 6 mm, the resulting stress in the compressive flange is lower than the critical stress, and the beam stiffness decreases linearly with respect to thickness reduction. Thin-walled beams have high material effectiveness, leading to more and more uniform distributions of internal loads. Accordingly, λ values decrease as thickness decreases in the pre-buckling stage.

In the post-buckling stage as thickness reduction proceeds from around 6 mm, buckling occurs in the compressive flange and causes a further reduction in beam stiffness, as shown in **Figure 6(a)**. Stress distribution becomes more and more non-uniform and the material in the central region of the compressive flange becomes less effective in sustaining loadings. **Figure 6(b)** shows the corresponding variations of λ and it is obvious the λ values increase, due to the buckling in the compressive flange, as thickness reduction proceeds.

4. Conclusion

This paper investigates the effect of local buckling on the gauge sensitivity index of thin-walled beams. It has been illustrated λ values decrease with decreasing of thickness in the pre-buckling stage. At very thin component thickness, however, the onset of local buckling results in a loss of effective length in the compressive segments. The effect of buckling on the λ values has been analyzed based on the effective width method and it has been illustrated λ values will increase due to non-uniform stress distributions in the post-buckling stage. Nonlinear FEA are conducted for a thin-walled beam to validate the effect of local buckling on changes of gauge sensitivity. Bending stiffness has been first calculated for the beam with different thickness ranging from 10 mm to 1 mm. Corresponding λ values are computed based on the obtained beam stiffness values in the pre- and post-buckling stages. It is found local buckling in the compressive beam component will lead to an increase in λ values, indicating the stress distribution changing from a uniform status in the pre-buckling stage to non-uniform status in the post-buckling stage. It is validated from the nonlinear FEA results that gauge sensitivity index can be used for indicating and measuring the onset and degree of compressive buckling in thin-walled beams. Further investigations in-

clude numerical validations of thin-walled beams with open cross sections.

Acknowledgements

This research is partially funded by PNW Catalyst Grant. The support is gratefully acknowledged. The author is also grateful to Roger Eduardo Ona Ona for assisting the research.

Conflicts of Interest

The author declares no conflicts of interest regarding the publication of this paper.

References

- [1] Kim, H.C. and Wallington, T.J. (2013) Life Cycle Assessment of Vehicle Lightweighting: A Physics-Based Model of Mass-Induced Fuel Consumption. *Environmental Science & Technology*, **47**, 14358-14366. <https://doi.org/10.1021/es402954w>
- [2] Kim, H.C. and Wallington, T.J. (2016) Life Cycle Assessment of Vehicle Lightweighting: A Physics-Based Model to Estimate Use-Phase Fuel Consumption of Electrified Vehicles. *Environmental Science & Technology*, **50**, 11226-11233. <https://doi.org/10.1021/acs.est.6b02059>
- [3] Geyer, R. and Malen, D. (2020) Parsimonious Powertrain Modeling for Environmental Vehicle Assessments: Part 1—Internal Combustion Vehicles. *International Journal of Life Cycle Assessment*, **25**, 1566-1575. <https://doi.org/10.1007/s11367-020-01774-0>
- [4] Geyer, R. and Malen, D. (2020) Parsimonious Powertrain Modeling for Environmental Vehicle Assessments: Part 2—Electric Vehicles. *The International Journal of Life Cycle Assessment*, **25**, 1576-1585. <https://doi.org/10.1007/s11367-020-01775-z>
- [5] Patrone, G.L., Paffumi, E., Otura, M., Centurelli, M., Ferrarese, C., Jahn, S., Brenner, A., Thieringer, B., Braun, D. and Hoffmann, T. (2022) Assessing the Energy Consumption and Driving Range of the QUIET Project Demonstrator Vehicle. *Energies*, **15**, 1290. <https://doi.org/10.3390/en15041290>
- [6] Bai, J., Zhao, Y., Meng, G. and Zuo, W. (2021) Bridging Topological Results and Thin-Walled Frame Structures Considering Manufacturability. *Journal of Mechanical Design*, **143**, Article ID: 091706. <https://doi.org/10.1115/1.4050300>
- [7] Czerwinski, F. (2021) Current Trends in Automotive Lightweighting Strategies and Materials. *Materials*, **14**, 6631. <https://doi.org/10.3390/ma14216631>
- [8] Burd, J.T.J., Moore, E.A., Ezzat, H., Kirchain, R. and Roth, R. (2021) Improvements in Electric Vehicle Battery Technology Influence Vehicle Lightweighting and Material Substitution Decisions. *Applied Energy*, **283**, Article ID: 116269. <https://doi.org/10.1016/j.apenergy.2020.116269>
- [9] Von Karman, T., Sechler, E.E. and Donnell, L.H. (1932) The Strength of Thin Plates in Compression. *Transaction ASME*, **54**, 54-55.
- [10] Hao, P., Yuan, X., Liu, C., Wang, B., Liu, H., Li, G. and Niu F. (2018) An Integrated Framework of Exact Modeling, Isogeometric Analysis and Optimization for Variable-Stiffness Composite Panels. *Computer Methods in Applied Mechanics and Engineering*, **339**, 205-238. <https://doi.org/10.1016/j.cma.2018.04.046>
- [11] Patton, R. and Edwards, M. (2002) Estimating Weight Reduction Effects of Material Substitution on Joints with Constant Stiffness. SAE Paper Number 2002-010368.

<https://doi.org/10.4271/2002-01-0368>

- [12] Prater, G., Zhang, S.Y., Shahhosseini, A. and Osborne, G. (2008) Application and Experimental Validation of Gauge Sensitivity Indices for Vehicle Body Structure Optimization. SAE Paper Number 2008-01-0883.

<https://doi.org/10.4271/2008-01-0883>